International Journal of Academic Information Systems Research (IJAISR)
ISSN: 2643-9026
Vol. 9 Issue 11 November - 2025, Pages: 36-48

Research and Comparison of Facial Color Normalization Methods Relative to an Etalon Image

Ivan Larin, Iryna Tvoroshenko, Volodymyr Gorokhovatskyi, Valentyn Liubchenko

Department of Informatics
Kharkiv National University of Radio Electronics,
Kharkiv, Ukraine
e-mail: ivan.kaziuta@nure.ua; iryna.tvoroshenko@nure.ua; volodymyr.horokhovatskyi@nure.ua; valentyn.liubchenko@nure.ua

Abstract: *This paper addresses the research of facial color normalization methods in images. The purpose of the research is to compare methods of normalizing facial color relative to an etalon image. The following methods were used for the research: Histogram matching, Color transfer, and Color transfer based on Face Parsing. The essence of the methods is demonstrated in detail by constructing block diagrams. The current application of normalization methods in applications and relevant literature sources is analyzed. The scientific novelty lies in the comparison of methods aimed at solving the problem of face color normalization relative to an etalon image, based on criterion descriptions. The research is based on the subject area and architecture studied and presented as a result of previous work. The application used is one of the microservices of the designed system. The results of this research can be used in practical tasks related to computer vision and, in particular, the processing of human face color in images or video frames. As a result of the research, an application was developed to normalize the color of faces relative to an etalon image using three methods, and the accuracy of the operations performed was calculated based on the corresponding criterion description.*

Keywords—algorithm; brightness; face normalization; face recognition; flowchart; illumination correction; OpenCV library; white balance

1. INTRODUCTION

The problem of facial recognition has existed since ancient times and is particularly relevant today in electronic access systems and biometrics. The identification result is greatly influenced by shooting conditions: lighting, background, clothing, makeup, and distance to the camera. Unlike humans, who can quickly adapt (move to a better-lit place, illuminate their face, etc.), automated systems often have limitations on the number of attempts or the time between restarts. Therefore, it is extremely important to normalize the image of the face in advance, in particular in terms of lighting and color, in order to reduce the number of errors during identification.

The study considers etalon-based normalization methods that adjust the current image to an etalon made under the best conditions. These include: Histogram matching, Color transfer (Reinhard et al.) and Color transfer based on Face Parsing.

Histogram matching aligns the histogram of the input image relative to the histogram of the etalon. Its advantage is its adaptability to a specific etalon, which ensures similarity in lighting style. The method is widely used in biometrics, medicine, and satellite image processing. The disadvantage is the risk of unnatural skin tones and a “plastic” appearance of the face when there are large differences between images.

Color transfer (Reinhard) works in Lab space, where brightness is separated from color. The method equalizes the mean values and standard deviations of the channels between the etalon and the current image, resulting in a more natural result with fewer artifacts. It is used in photo and video editing, cinematography, and biometrics. The disadvantages are related to the global nature of the transformation and the possible transfer of unwanted tones from the etalon.

Color transfer based on Face Parsing is an evolution of the previous approach: instead of global processing, the entire scene is divided into fragments (face segments, background, hair, etc.), and normalization is applied locally. This allows you to correct only the necessary areas (for example, only the skin of the face), reducing the influence of the background and clothing. Disadvantages: dependence on segmentation quality, possible artifacts at segment boundaries, and high computational complexity. The method is less versatile but valuable for specific tasks – DeepFake, face reenactment, generative models, VR/AR.

The choice of these three methods is justified by the fact that they represent different approaches to normalization: strict distribution adjustment (Histogram matching), balanced color and brightness transfer (Reinhard Color transfer), and segment-oriented normalization (Color transfer based on Face Parsing). This combination allows for a comprehensive assessment of how global and local approaches affect the accuracy and stability of face recognition.

Histogram matching is used in Photoshop (Match Color), ArcGIS, and medical platforms such as HistomicsTK and Digital Slide Archive.

Color transfer is implemented in tools such as DaVinci Resolve (Color Match), Capture One (Normalize), and biometric SDKs (e.g., Luxand FaceSDK).

Color transfer with Face Parsing is used in biometric systems, medical tasks, and generative models where it is necessary to bring the visual characteristics of different images as close as possible (DeepFake, face reenactment, VR/AR).

This set of methods creates a reliable basis for further experimental comparison and selection of the optimal approach to face normalization in variable lighting conditions.

2. Related Works

The literature review covers a number of approaches to color and lighting normalization, as well as style transfer for facial images and similar tasks.

In [1], a deep architecture is proposed for automatically coloring video line images according to an etalon color style. The model consists of a color transformation network and a temporal 3U network, uses an attention mechanism with non-local matching search and AdaIN to ensure global color consistency, demonstrating better video coloring quality than existing methods.

In [2], colorization of a line drawing according to an etalon is considered, and a new attention mechanism, Stop-Gradient Attention (SGA), is proposed, which eliminates gradient conflicts between attention branches. This has significantly improved FID and SSIM compared to baseline methods.

In [3] describes a training platform for coloring cartoon sketches based on the style of an etalon image. The architecture includes a color style extractor, a coloring network, and a multi-scale discriminator, providing better visual quality and style consistency than existing approaches.

In [4], the concept of Color Space Normalization (CSN) and two methods, CSN-I and CSN-II, are introduced, which normalize weak color spaces (RGB, XYZ, etc.) and increase their recognition ability to a level equal to or higher than that of "strong" spaces (I1I2I3, YUV, YIQ, LSLM) in the task of face recognition (FRGC, AR).

In [5], a method for normalizing the lighting of color face images based on the Fong lighting model and a 3D face model is proposed. The algorithm estimates the parameters of light sources, shadows, and reflections, which improves the stability of recognition to changes in lighting (low mean approximation error).

In [6], an automated approach to the classification of dermatological diseases based on color photos is presented: first, the intensity is normalized and the lesions are segmented, then classification is performed using DenseNet201, achieving high accuracy (≈95%).

In [7], face recognition under occlusion and heterogeneous lighting conditions is investigated using a combination of YCbCr, HSV, and Lab color models, which improves accuracy, detection rate, false positives, and precision on the AR and Color FERET datasets, as well as on our own dataset.

In [8], AniGAN is proposed – a GAN framework for converting a real portrait photo into an anime face, taking into account the specific style of the etalon anime image. The architecture ensures simultaneous transfer of style, color, texture, and local shape while preserving the global structure of the face, and reduces artifacts through special normalizations in the generator.

Thus, the review shows that current research is actively developing both classical and deep methods of color normalization, lighting, and style transfer, in particular based on etalon images [9–18]. This confirms the relevance of further work in the field of face color normalization and etalon-based approaches to improve recognition quality.

3. Histogram Matching Method

Histogram matching – etalon-based normalization method: brings the histogram of the analyzed image to the histogram of the etalon image. Works with global image characteristics (contrast, tonal balance) rather than individual pixels.

Advantages:

- Each image has its own etalon, there is no "universal" norm.
- Well suited for tasks where data set unification is important (biometrics, medicine, histology, etc.).
- Reduces noise and makes the result more stable.

Disadvantages:

- With large differences in lighting/color gamut, unnatural shades and artifacts may appear.
- The method is global, which can cause local details to be lost and the face to look "plastic".
- For the task of normalizing faces for biometric identification, good lighting is more important than the complete preservation of local nuances – this method is particularly useful here.

The Histogram matching method allows you to transfer global characteristics from one image to another by aligning the histogram indicators of the images:

Step 1 (optional): Pre-processing of images. When processing different images, or when the etalon and analyzed images differ significantly in size or other parameters, it is better to first bring them to a certain "normal" state in which the images will have the least differences in parameters that do not relate to color.

Step 2: Calculating histograms. For the analyzed (S) and etalon (R) images, histograms h_S and h_R are constructed, where the number of pixels is located on the Y-axis and the brightness level is located on the X-axis.

Step 3: Calculation of the Probability Density Function (*PDF*). After constructing histograms for each image, it is necessary to calculate the probability density function

$$PDF(i) = \frac{i}{N}, \quad (1)$$

where *i* is the brightness level; *N* is the corresponding number of pixels.

Step 4: Calculation of the Cumulative Distribution Function (*CDF*). After calculating the density function, it is necessary to calculate the cumulative distribution function of each image *i* using the following formula

$$CDF(i) = \sum_{j=0}^{i} PDF(j), \quad (2)$$

where *i* is the brightness level.

Step 5: Constructing a LookUp Table (*LUT*). To transfer characteristics from the reference image to the analyzed image, it is necessary to construct a lookup table.

The table is filled in according to the following principle: for each level *i* in image *R*, it is necessary to find such a value of level j in image *S* that *CDF(i)* is less than or equal to *CDF(j)*. When such a value is found, then *LUT[i] = j*.

Step 6: Apply the *LUT* to the output image. The final step in normalization is to transfer the corresponding values from image *R* to image *S*.

The new value of each pixel in the image is calculated as follows:

$$G(p) = LUT(CDF(p)), \quad (3)$$

where *p* is the value of the pixel in the image.

The algorithm of the histogram matching method is shown in Figure 1.

4. Color Transfer Method

Color transfer is one of the classic methods of transferring color between images. Its main idea is to first convert the image to *Lab* space and then transfer the values from the etalon space to the analyzed space.

Lab space is a way of transferring a color gamut using three variables: *L* – brightness, *a* – the ratio of green to red, *b* – the ratio of yellow to blue.

To transfer values between images, the common values μ – mean and σ – standard deviation are used.

That is, the color gamut of each pixel of the analyzed image in the *Lab* space will be changed according to these common etalon values.

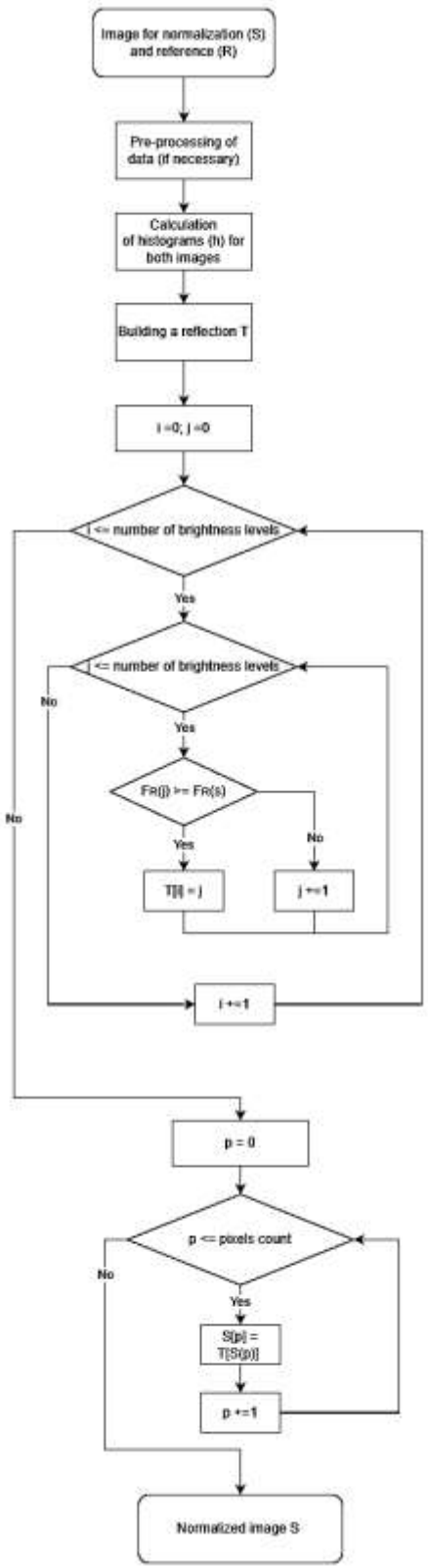

Fig. 1. *Step-by-step algorithm of the Histogram matching method*

The effectiveness of this approach lies in its high processing speed, since it is not necessary to change each pixel to individually calculated values. Also, due to the simplicity of the approach to transferring characteristics, it is easier to modify the algorithm by changing the degree of modification. An important drawback is the global nature of the calculation of characteristics, which excludes the influence of individual features of small areas in the image, which can lead to distortions. For example, a phenomenon such as a "gray veil" can occur, where the image loses contrast. Another problem can be areas that are too dark, too bright, or where one color significantly dominates the other colors in the image. Due to the global nature of the characteristics, their application can lead to incorrect transfer and distortion of the color gamut of the result.

Another disadvantage is the global nature of the method itself. Global characteristics applied to each pixel do not take into account the specifics of certain areas, in particular parts of the face, so even the absence of distortions does not guarantee that the parts of the face necessary for identification will be clearly visible in the output image.

The Color transfer method converts images from the *RGB* color space to *Lab*, whose transformations relative to the etalon allow you to obtain a normalized image. The method has a mandatory restriction on input data: input images must be in the *RGB* color space. Images can also be of different sizes.

A step-by-step algorithm of the Color transfer method is shown in Figure 2.

Step 1: Preprocessing of Images

If the input data is not in the *RGB* color space, it is necessary to convert the image from the corresponding space. Most often, the characteristics of a pixel in the *RGB* space are in the range [0, 255], where $C \in \{R, G, B\}$. In this case, the values must be made linear using the formula:

$$C'^{(i,j,k)} = \frac{C(i,j,k)}{255}, \quad (4)$$

where i is the pixel coordinate along the x-axis; j is the pixel coordinate along the y-axis; k is the channel type ($k \in \{R, G, B\}$); C' is the pixel value for channel k'; C is the original pixel value.

After that, it is necessary to remove the gamma using:

$$C_{lin} = \begin{cases} \frac{C'}{12{,}92} & C' \le 0{,}04045 \\ \left(\frac{C'+0{,}055}{1{,}055}\right)^{2{,}4} & C' > 0{,}04045 \end{cases}, \quad (5)$$

where $C' \in \{R', G', B'\}$; C_{lin} – linear pixel value for the channel.

If the image is too dark or too light, or if there are other distortions, it is recommended to remove them before converting the image to a linear form.

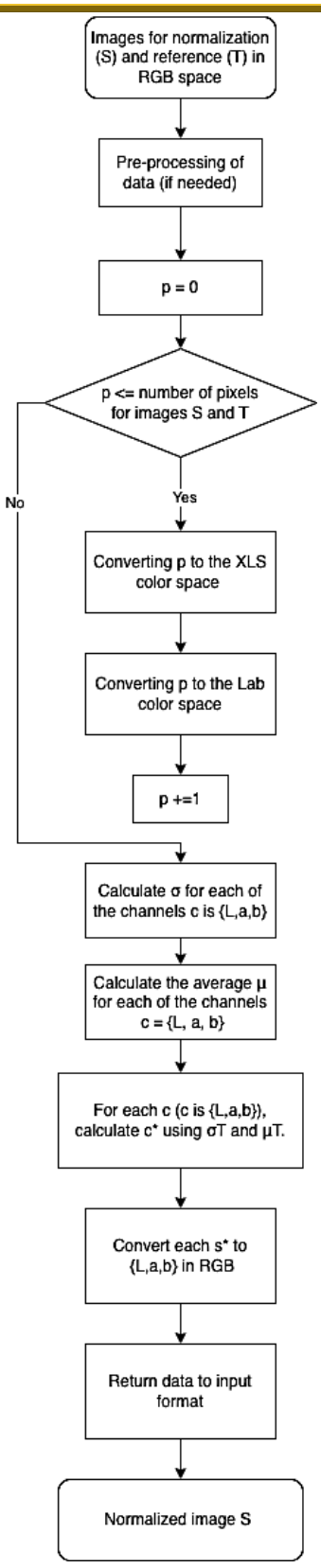

Fig. 2. *Step-by-step algorithm of the Color transfer method*

Step 2: Conversion to LMS Space

To convert an image to *Lab* space, you need to obtain an intermediate value in *LMS* space. The value of each pixel in the new space can be obtained using the following formula:

$$\begin{bmatrix} L \\ M \\ S \end{bmatrix} = \begin{bmatrix} 0{,}3811 & 0{,}5783 & 0{,}0402 \\ 0{,}1967 & 0{,}7244 & 0{,}0782 \\ 0{,}0241 & 0{,}1288 & 0{,}8444 \end{bmatrix} \begin{bmatrix} R \\ G \\ B \end{bmatrix}, \quad (6)$$

where *L*, *M*, *S* are the corresponding values of the *LMS* space; *R*, *G*, *B* are the linear values of the *RGB* space.

Step 3: Neutralization of Data Asymmetry (Optional)

To improve data accuracy, you can convert it to logarithmic form using:

$$k' = log\, k\,, \quad (7)$$

where *k'* is the logarithmic value of *k* ($k \in \{l, a, b\}$).

Step 4: Conversion to Lab Space

To transfer the color gamut characteristics, it is necessary to obtain the image values in *Lab* space. The following formula is used for conversion:

$$\begin{bmatrix} l \\ a \\ b \end{bmatrix} = \begin{bmatrix} \frac{1}{\sqrt{3}} & 0 & 0 \\ 0 & \frac{1}{\sqrt{6}} & 0 \\ 0 & 0 & \frac{1}{\sqrt{2}} \end{bmatrix} \begin{bmatrix} 1 & 1 & 1 \\ 1 & 1 & -2 \\ 1 & -1 & 0 \end{bmatrix} \begin{bmatrix} L \\ M \\ S \end{bmatrix}, \quad (8)$$

where *l*, *a*, *b* are the corresponding values of the *Lab* space variables; *L*, *M*, *S* are the corresponding linear values of the *LMS* space variables.

Step 5: Calculation of Global Characteristics

After obtaining the values of all pixels in the *Lab* space, it is necessary to calculate the values of the mathematical mean (μ) and the standard deviation (σ).

The characteristics can be calculated using the following formulas:

$$\mu^{(c)} = \frac{1}{N}\sum_{i \in N} I(i), \quad (9)$$

$$\sigma^{(c)} = \sqrt{\frac{1}{N}\sum_{i \in N}(I(i) - \mu)^2}, \quad (10)$$

where $c \in \{l, a, b\}$; *N* – number of pixels in the image; *I* – vector of pixel values in channel *c*.

Step 6: Transferring the Space from the Etalon Image to the Analyzed Image

The following formula is used to convert each pixel of the analyzed image

$$I_{S'}^{(c)} = \left(\frac{I_S^{(c)} - \mu_S^{(c)}}{max(\sigma_S^{(c)}, \varepsilon)}\right)\sigma_T^{(c)} + \mu_T^{(c)}, \quad (11)$$

where *c* is the channel value ($c \in \{l, a, b\}$); σ_R is the standard deviation for image *R* ($R \in [S, T]$); *S* is the analyzed image; *T* – etalon image; $\varepsilon = 10^{-6}$.

Step 7: Reverse Conversion to LMS Space

To obtain a normalized image, the modified pixels *S'* must be converted from *Lab* space to *RGB*. An intermediate conversion to *LMS* space can be obtained using the formula:

$$\begin{bmatrix} L' \\ M' \\ S' \end{bmatrix} = \begin{bmatrix} \frac{1}{\sqrt{3}} & \frac{1}{\sqrt{6}} & \frac{1}{\sqrt{2}} \\ \frac{1}{\sqrt{3}} & \frac{1}{\sqrt{6}} & -\frac{1}{\sqrt{2}} \\ \frac{1}{\sqrt{3}} & -\frac{1}{\sqrt{6}} & 0 \end{bmatrix} \begin{bmatrix} l' \\ a' \\ b' \end{bmatrix}, \quad (12)$$

where *l'*, *a'*, *b'* are the corresponding values of the *Lab* space variables in image *S'*; *L'*, *M'*, *S'* are the corresponding linear values of the *LMS* space variables in image *S'*.

Step 8: Conversion to Linear Form (Optional)

If the action in Step 3 was applied to reduce data dispersion, then to return to the original data form, it is necessary to convert the logarithm using the following:

$$k' = 10^k, \quad (13)$$

where *k'* is the linear value of *k*, where $k \in \{l', a', b'\}$.

Step 9: Conversion to RGB Space

To obtain a normalized result, the *LMS* space must be converted back to *RGB*. The following formula is applied to image *S'*:

$$\begin{bmatrix} R' \\ G' \\ B' \end{bmatrix} = \begin{bmatrix} 4{,}4679 & -3{,}5873 & 0{,}1193 \\ -1{,}2186 & 2{,}3809 & -0{,}1624 \\ 0{,}0497 & -0{,}2439 & 1{,}2045 \end{bmatrix} \begin{bmatrix} L' \\ M' \\ S' \end{bmatrix}, \quad (14)$$

where *L'*, *M'*, *S'* are the corresponding values of the *LMS* space of image *S'*; *R'*, *G'*, *B'* are the linear values of the *RGB* space of image *S'*.

Step 10: Convert Pixel Values to Non-Linear Values

To obtain data in the same format as it was at the input, it is necessary to perform the reverse of Step 1: return the gamma and convert the values to 8-bit format. The gamma is returned using the following formula:

$$C'^{(i,j,k)} = \begin{cases} 12{,}92\, C_{lin}' & C_{lin}'' \le 0{,}0031308 \\ 1{,}055 C_{lin}'^{1/2{,}4} - 0{,}55 & C_{lin}' > 0{,}0031308 \end{cases}, \quad (15)$$

where *i* is the pixel coordinate along the *x*-axis; *j* is the pixel coordinate along the *y*-axis; *k* is the channel type ($k \in \{R', G', B'\}$); C_{lin}' – linear value of the pixel along the *i* and *j* coordinates for channel *k*; *C* – value of the pixel with the returned gamma along the *i* and *j* coordinates for channel *k*.

If, after gamma correction, the data exceeds the range [0, 1], for example, if it is negative, then the following formula must be applied to all pixels:

$$C'(i,j,k) = min(1, max(0, C'(i,j,k)). \quad (16)$$

To convert to an 8-bit system, the following formula is used:

$$C''(i,j,k) = round(255 * C'(i,j,k)). \quad (17)$$

To stay within the range [0, 255], use this formula:

$$C''(i,j,k) = min(255, max(0, C''(i,j,k)). \quad (18)$$

After completing all stages, the obtained values of individual pixels are converted for display as an image.

5. Color Transfer Based on Face Parsing Method

Color transfer based on Face Parsing is a method that uses the method described above, working not with the entire image as a whole, but breaking it down into separate parts. For example, when working with a face, you can highlight its main areas, such as the nose, mouth, eyes, ears, and chin. This makes it possible to exclude areas that may not be important for specific tasks. For example, the most important areas for face recognition are the eyes, nose, and mouth.

After selecting the areas, the chosen color normalization method is applied to each of them separately. In the method considered in this work, the Color transfer method is used, but any other method can be used.

The main advantages and disadvantages of the approach coincide with the corresponding characteristics of the chosen face color normalization method. A distinctive feature of the method is that it works with the image in parts rather than as a whole, which can negate the negative effect of transferring global characteristics from the etalon image by filtering out unnecessary areas of the face, the calculation of which often results in errors in the characteristics, or greater accuracy in calculating the characteristics for the corresponding area, ignoring very bright or dark areas in other parts of the image.

One drawback is the inconsistency of the normalized areas of the face. Since the characteristics for each area are calculated separately and have no coordination or global characteristics, after normalization is complete, seams may appear that show the boundaries within which the segment was selected.

The Color transfer method based on Face Parsing highlights areas on the face and converts each of them from the RGB color space to Lab, the collage of transformations of which relative to the etalon allows you to obtain a normalized image. If there are several faces in the image, the one with the highest model confidence is processed; if no face is found, the input image is returned unchanged.

To implement the method considered in this work, the Media Pipe Face Mesh model [19] is used to recognize facial areas.

The following steps describe the algorithm of the method.

Step 1: Preliminary Data Processing

For each image *I*, the model returns *N* normalized two-dimensional coordinates according to the formula:

$$P = \{(x_i, y_i) \in [0,1]^2\}_{i=1}^{N}. \quad (19)$$

You need to convert them to pixel coordinates using the following formulas:

$$X_i = [x_i W], \quad (20)$$

$$Y_i = [y_i H], \quad (21)$$

where *H* is the height of the image; *W* is the width of the image.

Form a set of semantic zones *K*. The model used employs the following set: *K* = {lips, left_eye, right_eye, left_brow, right_brow, nose, face_oval}.

Step 2: Construct Polygonal Masks for the Zones

For each zone *k*, calculate the set of etalon points in pixel space using the formula:

$$Q(k) = \{(X_i Y_i) : i \in I_k\}, \quad (22)$$

where I_k are pixels belonging to region *k* in image *I*.

Then, for each region *k*, it is necessary to calculate the convex hull (H_k).

After obtaining the convex hull, it is necessary to determine the binary mask polygon using the formula:

$$M_k(x,y) = \begin{cases} 1, & (x,y) \in H_k \\ 0, & (x,y) \notin H_k \end{cases}. \quad (23)$$

Step 3: Morphological Stabilization of Small Areas (Optional)

If there are areas with high detail, such as eyes, lips, nose, eyebrows, it is recommended to apply erosion with a radius of [1, 2] to eliminate the capture of small background areas. The following formula is used to select K_{small} areas:

$$M'_k = \varepsilon_{p_k}(M_k). \quad (24)$$

Step 4: Creating a Skin Mask

To separate the skin from the nose, eyes, and eyebrows, you need to create a skin mask and use it to transform the masks for each of the areas. To create a skin mask, use the following formula:

$$M_{skin} = M_0 \vee \ldots \vee M_{n-1}, \quad (25)$$

where *n* is the number of elements in the set K_{small}.

The following formula is used to obtain the primary skin mask:

$$M'_{skin} = (M_{face_oval} - M_{skin}). \quad (26)$$

After obtaining the initial skin mask, the M_{face_oval} value must be replaced with M'_{skin}.

Step 5: Forming a Set of Masks

At this stage of the method, the plane of the area is checked to reject areas that are too small. After that, it is necessary to form a set of ready-made masks.

Preliminary list of areas for filtering:

$S = \{M_{lips}, M_{left_eye}, M_{right_eye}, M_{left_brow}, M_{right_brow}, M_{nose}, M_{skin}\}$.

Filtration of areas is performed according to the formula:

$$\sum_{(x,y) \in I} M(x,y) \geq T, \quad (27)$$

where T is the number of pixels that limit the plane of the area; $M \in S$.

Step 6: Forming the Order of Areas

To reduce the likelihood of distortion during color normalization of the analyzed area, it is recommended to form an order in which the areas will undergo normalization.

First, small and contrasting structures (lips, eyes, eyebrows) are normalized so that their color is not captured by other areas during further merging. The nose is processed before the "skin" because it combines both smooth and sharp transitions. The "skin" is processed last as the largest area, which "picks up" the remaining differences and minimizes global seams.

In case of mask intersection, the area that is later in the queue (according to the specified order) has priority, which minimizes visible seams on large areas of skin.

For the list of masks S considered, the order will be as follows:

lips → left_eye → right_eye → left_brow → right_brow → nose → skin.

Step 7: Application of the Color Transfer Algorithm

For each mask area from S, the corresponding algorithm is applied in the established order.

After obtaining the normalized region, the final image is updated: pixels where $M_k = 1$ is replaced with normalized values; outside the mask, the previous state is preserved.

After color normalization is complete in all regions of the image, it is considered normalized.

A step-by-step algorithm for the Color transfer method based on Face Parsing is shown in Figure 3.

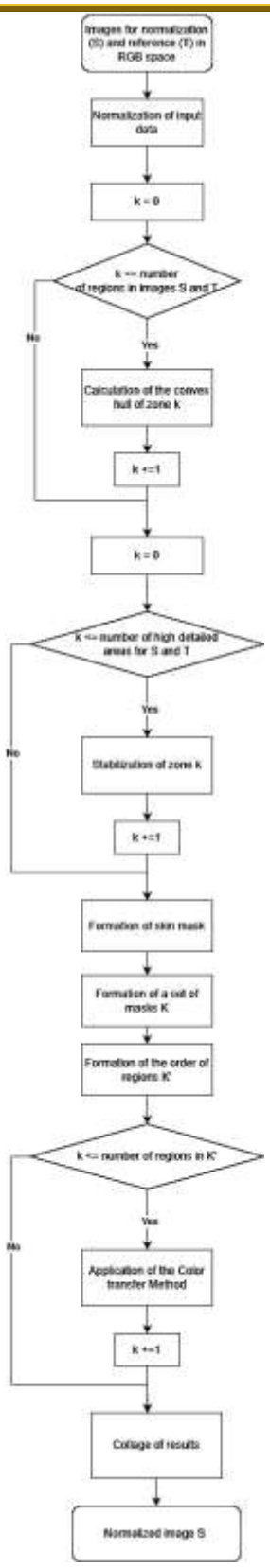

Fig. 3. *Step-by-step algorithm of the Color Transfer method based on Face Parsing*

International Journal of Academic Information Systems Research (IJAISR)
ISSN: 2643-9026
Vol. 9 Issue 11 November - 2025, Pages: 36-48

6. EXPERIMENTS

After practical implementation of the Histogram matching, Color transfer, and Color transfer based on Face Parsing methods, experiments were conducted using them to normalize face color relative to the etalon method.

To demonstrate the results, five images were taken from each of the three classes (Extended Yale B dataset [20]) and normalized using the methods described above.

For each image, after normalization using one of the methods, a "before" and "after" collage was created, where the first image is the analyzed one, and the second is the result of normalization. Examples of face color normalization for image 11 [20] of class 1 using the methods considered are shown in Figures 4–6.

Fig. 4. *Result of image normalization 11 from class 1 using the Histogram matching method (input (left) and normalized (right) images)*

Fig. 5. *Result of image normalization 11 from class 1 using the Color transfer method (input (left) and normalized (right) images)*

Fig. 6. *Result of image normalization 11 from class 1 using the Color transfer method based on Face Parsing (input (left) and normalized (right) images)*

7. TESTING

After normalizing all images from all three classes, the accuracy of each method was evaluated.

The evaluation was performed by calculating the following characteristics separately for each class:

- SSIM.
- Bhattacharyya.
- Gray-World angle.
- ΔE^*ab.
- Contrast error L.
- Clipping (black + white).

The characteristics were calculated by comparing the normalized image to the etalon of the corresponding class.

The calculated indicators for the first class are shown in Figure 7.

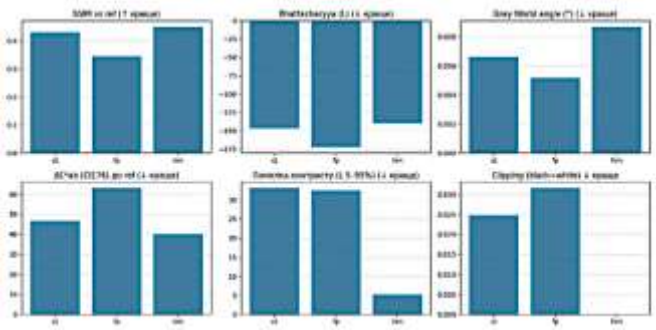

Fig. 7. *Metric estimates of normalization accuracy on class 1 images*

The data obtained shows that for most characteristics (except Bhattacharyya and Gray-World angle), the Histogram matching method performed best in class 1.

According to the SSIM assessment, Color transfer was close to the Histogram matching result. The advantage of Color transfer based on Face Parsing in terms of Bhattacharyya and Gray-World angle can be explained by the method preserving the original histogram, which will be more similar to the etalon histogram.

Histogram matching, in turn, by adjusting the histogram to the etalon, can change its shape. In the case of Gray-World angle, Color transfer based on Face Parsing has a significant impact on colors, not just brightness. When normalized using Histogram matching, the color shift is preserved, which affects the indicator.

Figure 8 shows the metric data for class 2.

The results of class 2 analysis show similarities with the previous class.

The difference between the new results lies in the almost equal SSIM values for the Color transfer and Histogram matching methods.

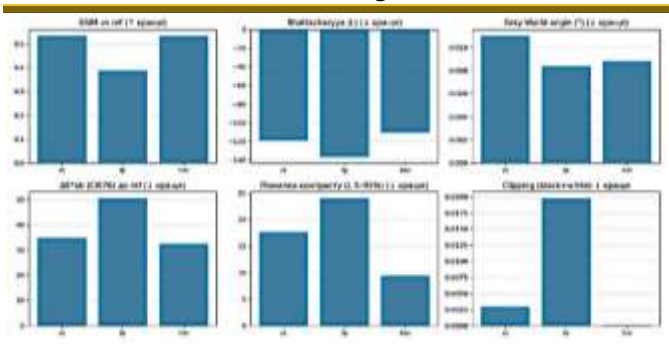

Fig. 8. *Metric estimates of normalization accuracy on class 2 images*

The difference between Face Parsing-based Color transfer and Histogram matching on class 2 elements has decreased. This may be due to differences in the natural skin colors of the people whose photos were examined.

Unlike class 1 images, the Clipping indicator for Histogram matching has increased, which may indicate greater data loss in the dataset.

The results of the analysis of class 3 images are shown in Figure 9.

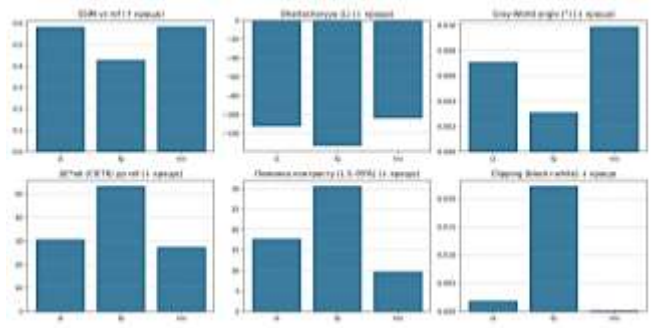

Fig. 9. *Metric estimates of normalization accuracy on class 3 images*

The results show that the Histogram matching problems already seen in the previous classes remain.

Although there is still a small difference in the SSIM scores for the Histogram matching and Color transfer methods in the current class, the Bhattacharyya and Gray-World angle scores for Histogram matching are similar to those for class 1.

This section discusses the results of comparing original and normalized images relative to the etalon using the methods discussed in [19]. The original images are shown on the left side of Figures 4–6. Each image was compared only with the etalon image of its class.

Table 1 shows the results of comparing the original images with the etalon images.

The data obtained show that images with a relatively high level of illumination, for example, 13, 16, and 39, have a high degree of similarity, even without additional normalization. At the same time, images with a low level of illumination show high results only with the FaceNet method, which may indicate the need for its further improvement.

Table 2 shows the results of comparing images normalized using the Histogram matching method.

The results of comparing normalized images show an increase in the degree of similarity. The indicators for images that did not have a high level of illumination increased particularly significantly. After normalization, they can be identified with high accuracy (>90%), and only in two cases is the similarity of images below this threshold.

Table 3 shows the results of comparing images normalized using the Color transfer method.

There is an increase in the degree of similarity after normalization, but it is lower than the values obtained using the Histogram matching method.

A sharp increase in the similarity percentage was recorded for images with low lighting levels, in particular for image 11 in classes 1 and 3 (by approximately 19% in both cases).

For image 11 in class 2, the degree also increased, but it is still within the low similarity range.

The average similarity degree (90.66%) after normalization using the Color transfer method can be considered high, but it is significantly inferior to the Histogram matching method with an average similarity degree (94.5%).

Table 4 shows the comparison results after normalization using the Color transfer method based on Face Parsing.

The results show that further work is needed to improve the Color transfer method based on Face Parsing, as normalization was able to significantly increase (by several percent) the degree of similarity for only three images (13, 16, and 39 for class 1).

In other cases, the similarity level remained the same or showed a slight increase (up to 0.4%). In the case of images 13 and 39 in class 3, the similarity percentage decreased significantly (by 5%–7%).

The average similarity level for the Color transfer method based on Face Parsing also remains significantly lower than the previous methods (84.8%) and does not differ much from the initial one (83.57%). The reason for such low performance of the method may be poor mutual adjustment of the face recognition model and the color normalization method.

Table 1: Results of Comparing Original Images to Etalon Images

Class name	Picture number	Percentage of image similarity (%)			Average similarity (%)
		Eigenfaces	FaceNet	OpenFace	
Person 1	11	34.65	85.55	83.64	67.95
	13	86.91	97.18	96.55	93.55
	16	76.74	89.52	92.32	86.19
	29	95.15	9.34	98.93	97.81
	39	69.56	94.43	90.13	84.71
Person 2	11	1.32	77.81	80.4	53.18
	13	96.59	98.5	96.97	97.35
	16	77.9	99.16	97.29	91.45
	29	28.15	85.53	85.71	66.46
	39	90.5	98.6	99.3	96.13
Person 3	11	25.5	91.71	80.39	65.87
	13	93.9	99.08	98.33	97.1
	16	78.03	98.7	95.66	90.8
	29	40.36	88.03	79.5	69.3
	39	95.6	96.97	94.68	95.75

Table 2: Results of Comparing Images Normalized Using the Histogram Matching Method to Etalon Images

Class name	Picture number	Percentage of image similarity (%)			Average similarity (%)
		Eigenfaces	FaceNet	OpenFace	
Person 1	11	93.9	94.91	94	94.27
	13	95.96	99.29	97.9	97.72
	16	92.85	96.59	95.53	94.99
	29	97.6	99.56	98.37	98.51
	39	91.74	97.12	96.07	94.98
Person 2	11	97.31	98.16	97.64	97.7
	13	96.65	97.76	97.97	97.46
	16	79.58	88.05	88.63	85.42
	29	89.96	98.78	99.24	95.99
	39	90.43	96.45	89.46	92.11
Person 3	11	95.63	99.09	95.61	96.78
	13	93.65	97.62	94.74	95.34
	16	80.13	94.69	83.33	86.05
	29	96.33	97.67	94.94	96.31
	39	93.9	94.91	94	94.27

Thus, after analyzing the results of the accuracy assessment of the selected normalization methods, we can conclude that the Histogram matching method is best suited for the problem of image color normalization with subsequent similarity assessment to the etalon, even under conditions of low performance when compared using Bhattacharyya and Gray-World angle.

As part of the work, a study of methods for normalizing face color relative to an etalon was conducted by developing a microservice desktop application that allows you to obtain a normalized image using the input image being analyzed and the etalon [21–23].

An analysis of literature sources on the application of various methods of color normalization in images was carried out, which made it possible to assess the current state of development of the issue.

An analysis of modern methods of color normalization relative to the etalon was carried out, which made it possible to identify and evaluate promising methods for further detailed consideration.

As part of the work, the methods of histogram matching, color transfer, and color transfer based on face parsing were investigated, which made it possible to describe a step-by-step algorithm for each of them.

Table 3: Results of Comparing Images Normalized Using the Color Transfer Method to the Etalon Images

Class name	Picture number	Percentage of image similarity (%)			Average similarity (%)
		Eigenfaces	FaceNet	OpenFace	
Person 1	11	88.71	86.04	88.20	87.65
	13	94.61	98.61	96.58	96.60
	16	90.52	92.55	92.47	91.85
	29	97.56	99.55	98.71	98.61
	39	88.51	95.19	88.76	90.82
Person 2	11	27.03	78.61	80.30	61.98
	13	97.36	98.63	97.45	97.81
	16	96.74	98.93	98.59	98.09
	29	76.86	85.85	85.21	82.64
	39	90.43	98.55	99.22	96.07
Person 3	11	88.81	89.49	81.90	86.73
	13	95.67	98.94	97.09	97.23
	16	93.87	98.91	94.91	95.90
	29	78.17	85.82	82.38	82.12
	39	96.43	97.67	93.38	95.83

Table 4: Comparison Results of Images Normalized Using the Color Transfer Method Based on Face Parsing to the Etalon Images

Class name	Picture number	Percentage of image similarity (%)			Average similarity (%)
		Eigenfaces	FaceNet	OpenFace	
Person 1	11	89.22	86.60	83.09	86.30
	13	95.27	96.21	94.16	95.21
	16	91.74	89.51	85.84	89.03
	29	97.53	99.49	98.22	98.41
	39	89.50	93.36	88.53	90.46
Person 2	11	1.32	77.81	80.40	53.18
	13	96.60	98.49	96.98	97.36
	16	78.05	99.14	97.29	91.49
	29	28.38	85.45	85.71	66.51
	39	90.53	98.60	99.30	96.14
Person 3	11	25.50	91.71	80.39	65.87
	13	92.95	94.84	85.44	91.08
	16	78.03	98.70	95.66	90.80
	29	40.36	88.03	79.50	69.30
	39	93.81	94.31	84.78	90.97

8. CONCLUSION

The algorithms of the methods were visualized by constructing block diagrams, which made it possible to depict each step and create a software implementation for testing on a data set. It was established that for the task of face normalization when comparing with another image, the Histogram matching method is preferable.

Based on the Extended Yale B dataset [20], a proprietary test dataset was formed with 3 classes (images of 3 people) with 56 elements in each, where an element is a photo of a person under different lighting conditions.

The formed set allowed us to evaluate the performance of the methods under different lighting conditions and with different facial features.

We developed the ability to test by calling the application API, which allowed us to check the system and get the result without the need to launch other microservices.

The scientific novelty lies in identifying opportunities to use the method of color distribution alignment using histograms, as well as transferring the *Lab* space by dividing the face into segments for further face identification and providing access to the system.

The practical significance of the research lies in:

- Forming an approach to the preliminary normalization of biometric data.
- Increasing the reliability and accuracy of identification under different lighting conditions.
- Researching the use of methods in computer vision applications for image normalization.

9. ACKNOWLEDGMENT

The papers acknowledge the support of the Department of Informatics, Kharkiv National University of Radio Electronics, Ukraine, in numerous help and support to complete this paper.

The research results were obtained as part of the EU Horizon Europe international research project INITIATE (grant No. 101136775).

10. REFERENCES

[1] Shi, M., Zhang, J. Q., Chen, S. Y., Gao, L., Lai, Y. K., & Zhang, F. L. (2022). Reference-based deep line art video colorization, IEEE Trans. Vis. Comput. Graph., vol. 29, no. 6, pp. 2965-2979.

[2] Li, Z., Geng, Z., Kang, Z., Chen, W., & Yang, Y. (2022). Eliminating gradient conflict in reference-based line-art colorization, in Eur. Conf. Comput. Vis., pp. 579-596.

[3] Liu, X., Wu, W., Li, C., Li, Y., & Wu, H. (2022). Reference-guided structure-aware deep sketch colorization for cartoons, Comput. Vis. Media, vol. 8, no. 1, pp. 135-148.

[4] Yang, J., Liu, C., & Zhang, L. (2010). Color space normalization: Enhancing the discriminating power of color spaces for face recognition, Pattern Recognit., vol. 43, no. 4, pp. 1454-1466.

[5] Al-Osaimi, F. R., Bennamoun, M., & Mian, A. (2006). Illumination normalization for color faces images, in Int. Symp. Vis. Comput., pp. 90-101.

[6] Goceri, E. (2021). Deep learning-based classification of facial dermatological disorders, Comput. Biol. Med., vol. 128, p. 104118.

[7] Kumar, A., Kumar, M., & Kaur, A. (2021). Face detection in still images under occlusion and non-uniform illumination, Multim. Tools and Appl., vol. 80, no. 10, pp. 14565-14590.

[8] Li, B., Zhu, Y., Wang, Y., Lin, C. W., Ghanem, B., & Shen, L. (2021). Anigan: Style-guided generative adversarial networks for unsupervised anime face generation, IEEE Trans. Multim., vol. 24, pp. 4077-4091.

[9] Gorokhovatskyi, V., Tvoroshenko, I., Kobylin, O., and Vlasenko, N. (2023). Search for visual objects by request in the form of a cluster representation for the structural image description, Adv. Electr. Electron. Eng., vol. 21, no. 1, pp. 19-27.

[10] Pomazan, V., Tvoroshenko, I., & Gorokhovatskyi, V. (2023). Development of an application for recognizing emotions using convolutional neural networks, Int. J. Acad. Inf. Syst. Res., vol. 7, no. 7, pp. 25-36.

[11] Pomazan, V., Tvoroshenko, I., & Gorokhovatskyi, V. (2023). Handwritten character recognition models based on convolutional neural networks, Int. J. Acad. Eng. Res., vol. 7, no. 9, pp. 64-72.

[12] Gorokhovatskyi, V., Tvoroshenko, I. & Yakovleva, O. (2024). Transforming image descriptions as a set of descriptors to construct classification features, Indones. J. Elec. Eng. Comput. Sci., vol. 33, no. 1, pp. 113-125.

[13] Tvoroshenko, I., Gorokhovatskyi, V., Kobylin, O., & Tvoroshenko, A. (2023). Application of deep learning methods for recognizing and classifying culinary dishes in images, Int. J. Acad. Appl. Res., vol. 7, no. 9, pp. 57-70.

[14] Gorokhovatskyi, V., Tvoroshenko, I., Yakovleva, O., Hudáková, M., & Gorokhovatskyi, O. (2024). Application a committee of Kohonen neural networks to training of image classifier based on description of descriptors set, IEEE Access, vol. 12, pp. 73376-73385.

[15] Daradkeh, Y. I., Gorokhovatskyi, V., Tvoroshenko, I., Gadetska, S., & Al-Dhaifallah, M. (2023). Statistical data analysis models for determining the relevance of structural image descriptions, IEEE Access, vol. 11, pp. 126938-126949.

[16] Bohdan, N., Tvoroshenko, I., Gorokhovatskyi, V., and Kobylin, O. (2025). Development of a hybrid method to enhance context memory for a chatbot application based on large language models, Int. J. Acad. Inf. Syst. Res., vol. 9, no. 10, pp. 7-18.

[17] Suprun, A., Tvoroshenko, I., Gorokhovatskyi, V., and Yakovleva, O. (2025). Development and research of a method for the combined use of large language models for text generation, Int. J. Acad. Appl. Res., vol. 9, no. 10, pp. 249-263.

[18] Tvoroshenko, I., Pomazan, V., Gorokhovatskyi, V., & Kobylin, O. (2023). Application of video data classification models using convolutional neural networks, Int. J. Acad. Appl. Res., vol. 7, no. 11, pp. 134-145.

[19] MediaPipe Face Mesh. [Online]. Available: https://mediapipe.readthedocs.io/en/latest/solutions/face_mesh.html.

[20] Bourton, T. (2020). ExtYaleBCroppedPNG. The Extended Yale Face Database B Cropped. [Online]. Available: https://www.kaggle.com/datasets/tbourton/extyalebcroppedpng.

[21] Daradkeh, Y. I., Gorokhovatskyi, V., Tvoroshenko, I., and Zeghid, M. (2024). Improving the effectiveness of image classification structural methods by compressing the description according to the information content criterion, Comput. Mater. Contin., vol. 80, no. 2, pp. 3085-3106.

[22] Gorokhovatskyi, V., Chmutov, Y., Tvoroshenko, I., and Kobylin, O. (2025). Reducing computational costs by compressing the structural description in image classification methods, Adv. Inf. Syst., vol. 9, no. 1, pp. 5–12.

[23] Gorokhovatskyi, V., Tvoroshenko, I., Yakovleva, O., & Hudáková, M. (2025). Image description compression in classification structural methods, IEEE Access, vol. 13, pp. 43631-43641.